Proc. of the European Safety and Reliability Conference (ESREL 2026)
Edited by José C. Matos, Paulo B. Lourenço, Michael Beer, Daniel Oliveira, Edoardo Patelli, Hélder S. Sousa, Rui A. Silva and Monica Santamaria

doi: 10.3850/ESREL2026061419_esrel26-p27715-cd

Multi-criteria optimization of budget allocation for resilience improvement of interdependent critical infrastructures exposed to natural hazards

Santiago Taguado Menza

Department of Energy, Politecnico di Milano, Via la Masa 34, 20156, Milano, Italy. E-mail: santiago.taguado@polimi.it

Thomas Matteo Coscia

Department of Energy, Politecnico di Milano, Via la Masa 34, 20156, Milano, Italy. E-mail: thomasmatteo.coscia@polimi.it

Stefano Marchetti

Department of Energy, Politecnico di Milano, Via la Masa 34, 20156, Milano, Italy. E-mail: stefano.marchetti@polimi.it

The resilience of interdependent Critical Infrastructures (CIs) can be strengthened through targeted investments to mitigate the economic and social consequences of disruptive natural hazards. The optimal allocation of limited resources is challenged by the dynamic and conflicting preferences of decision-makers, as well as by the uncertainty associated with Climate Change (CC). In this work, the budget allocation problem is formulated as a Sequential Decision Problem (SDP), which is solved with Deep Reinforcement Learning (DRL) to identify the investment policy that minimizes the expected losses caused by disruptive events and the investments cost during the CIs lifetime. The novelty of the approach lies in the integration of: *i*) multi-criteria decision making to account for evolving stakeholder preferences within the SDP, *ii*) the probabilistic modelling of investments effectiveness according to CIs response to CC-induced natural hazards. The framework is applied to interdependent power and gas networks subject to coastal flood-induced disruptions. Results show that the method adapts to changes in stakeholder preferences as well as changes in natural hazards intensity, providing a flexible approach for resilience-oriented investment planning under uncertainty.

Keywords: *Critical Infrastructures (CIs), Resilience, Sequential Decision Problem (SDP), Climate Change (CC), Deep Reinforcement Learning (DRL).*

1. Introduction

Critical Infrastructures (CIs) are networks of heterogeneous systems (e.g., gas and water pipelines, electric grid) that provide essential commodities and services. Because of their interdependency, CIs are exposed to cascading failures, exacerbated by the increasing severity and frequency of extreme natural hazards (e.g., floods, droughts, landslides, and forest fires) due to Climate Change (CC) (Ouyang 2014). Thus, resilience, i.e., the capacity to absorb and recover from such events, is key. As a result, long-term investment planning targeted at enhancing CIs resilience focuses on proactive decisions (e.g., hardening, upgrades, redundancy) to reduce future disruptions and accelerate recovery (Fang et al. 2019).

Choosing an efficient sequence of resilience improvement actions is a challenging decision-making problem due to: *i*) the limited budget allocated, which is typically subdivided on a multi-decadal time scale, *ii*) the stochastic response of CIs to improvement actions, and *iii*) the dynamic evolution of stakeholder preferences during such long-term investment horizon (Nozhati 2021). Therefore, adaptive sequential decision-making frameworks that integrate multiple models (e.g., CI, natural hazard, fragility, recovery actions) to explore the consequences of extreme events and capture the non-stationary effects of CC on hazard frequency and intensity as well as changes in stakeholder preferences are essential.

Conventional approaches mainly use various optimization methods (e.g., dynamic programming, approximate dynamic programming) to derive near-optimal recovery and investment decisions under time-dependent resource constraints. Examples include stochastic and multi-level investment optimization recovery planning under hazard and climate uncertainty (Nozhati 2020). However, they are limited to discrete state and action spaces, and the solutions may not generalize beyond the optimization conditions.

To address these limitations, Deep Reinforcement Learning (DRL) has been used to enhance recovery policies by use of transfer learning to reduce the training burden for scenarios outside training conditions (Liang et al. 2026). However, existing DRL studies do not address both the changing stakeholder preferences over time and climate-driven non-stationarity.

We propose a novel adaptive DRL policy for sequential resilience investment planning that integrates multi-criteria preferences into the reward function and accounts for CC-driven hazard uncertainty through a probabilistic evaluation of investment effectiveness. The approach is demonstrated on a realistic case study of interdependent power and gas networks exposed to coastal flooding. Results show that the learned policy adapts to evolving preferences and improves resilience outcomes under uncertainty.

2. Proposed framework

The proposed framework consists of: *i*) a network-based model of the interdependent CIs which account for cascading failures (Section 2.1), *ii*) a copula-based model of the time dependent hazard intensity-duration relationship (Section 2.2), *iii*) a DRL based optimization of the budget allocation scheduling for resilience improvement (Section 2.3).

2.1. *Critical infrastructure model*

We consider a set of interdependent CIs indexed by $i = 1,2,\dots,I$. Each i-th CI is modeled as a directed graph:

$$G_i = (N_i, E_i) \tag{1}$$

where N_i is the set of nodes and $E_i \subseteq N_i \times N_i$ is the set of directed edges internal to the i-th CI. Interdependencies are modeled through directional edges between different CIs, which for any couple (i, j), with $j \in \{1,2,\dots,I\}$ and $j \neq i$, are defined as:

$$E_{(i\rightarrow j)} \subseteq N_i \times N_j \tag{2}$$

The overall interconnected CIs model is obtained by combining G_i and $E_{(i\rightarrow j)}$ $\forall i \neq j$, into a directed multilayer network (Clavijo Mesa et al. 2025).

Nodes are assumed to potentially fail due to a Disruptive Event (DE) of intensity H. Thus, for each node $n \in N_i$, a fragility function $\mathcal{F}_i^n$ is defined, so that the probability of node failure can be defined as:

$$\mathbb{P}(x_i^n = 0 \mid H) = \mathcal{F}_i^n(H) \tag{3}$$

Where $x_i^n \in \{0,1\}$ is a Boolean variable representing the n-th node post-DE state (0 failed, 1 working). Edges do not fail directly; instead, a directed edge is removed when one of its endpoint nodes fails. Consequently, nodes that are not directly failed can be disrupted by the loss of directed edges.

For each i-th CI, the magnitude of the disruption is quantified as the reduction of the supplied demand $U_{im} \in [0,1]$ due to the loss of connectivity between supplier nodes $N_i^s \subset N_i$ and consumer nodes $N_i^c \subset N_i$ ($N_i = N_i^s \cup N_i^c$), where $m = 1, 2, \dots, M$ index the considered consumer categories. Let us define d_{im}^c as the demand associated with the m-th consumer category supplied by the c-th consumer node of the i-th CI, with $c = 1, 2, \dots, |N_i^c|$, and the Boolean variable $z_i^c \in \{0,1\}$ (equal to 1 if consumer c is supplied after the DE) as:

$$z_i^c = 1\{x_i^c = 1 \wedge \exists s \in N_i^s : s \rightsquigarrow c\} \tag{4}$$

where $s \rightsquigarrow c$ denotes the existence of at least one directed path from any supplier node $s \in N_i^s$ to the c-th consumer node in the post-DE network. Then, the fraction of supplied demand is:

$$U_{im}(H) = \frac{\sum_{c=1}^{|N_i^c|} d_{im}^c \, z_i^c}{\sum_{c=1}^{|N_i^c|} d_{im}^c} \tag{5}$$

If all the consumer nodes are correctly supplied, i.e., $z_i^c = 1 \; \forall c \in N_i^c$, then $U_{im} = 1$. When a node fails, the associated restoration time T_i^n is modeled as the DE event duration T_H plus a repair time T_i^{nr} :

$$T_i^n = T_H + T_i^{nr}, \quad T_i^{nr} \sim f_i^n(\cdot) \tag{6}$$

where $f_i^n(\cdot)$ is the specific repair-time Probability Density Function (PDF) of the n-th node. We assume that all repair actions start at the same time, so that the disruption experienced by the m-th consumer category due to the DE is evaluated as:

$$D_{im}(H) = \left(1 - U_{im}(H)\right) \max_n(T_i^n) \tag{7}$$

2.2. *Natural hazard model*

In this work, DE caused by natural hazards are of interest. For the sake of performing resilience assessment, a natural hazard can be characterized by a pair of random variables, namely: *i*) hazard intensity $H > 0$ and *ii*) the associated duration time $T_H > 0$. These variables are typically positively correlated (i.e., more severe events tend to persist longer), hence their joint modelling should not assume independence. The marginal Cumulative Distribution Functions (CDFs) of H and T_H are estimated from historical data $\mathcal{Y}$ using standard univariate inference, so that:

$$F_H(h) = \mathbb{P}(H \leq h), F_{T_H} = \mathbb{P}(T_H \leq t_h) \tag{8}$$

with associated PDFs $f_H(h)$ and $f_{T_H}(t_h)$, respectively. Dependence between H and T_H is quantified via correlation measures (Kendall's τ and Spearman's ρ) estimated from $\mathcal{Y}$ and modelled through a copula function $\mathcal{C}(\cdot): [0,1]^2 \to [0,1]$. The joint CDF is given by Sklar's theorem as:

$$F_{H,T_H}(h, t_h) = \mathcal{C}\left(F_H(h), F_{T_H}(t_h), \vartheta\right) \tag{9}$$

where ϑ are the copula parameters. At discrete future times T_k indexed by $k = 1, 2, \dots, K$, correlated realizations of (h_k, t_{hk}) are generated as follows. For each T_k, a pair $(u_k, v_k) \in [0,1]^2$ is sampled from $\mathcal{C}(\cdot)$ (Salvadori and De Michele 2004) and by applying the probability integral transform theorem, we obtain:

$$h_k^0 = F_H^{-1}(u_k), \; t_{hk} = F_{T_H}^{-1}(v_k) \tag{10}$$

To include non-stationarity (CC and anthropogenic effects), an additive time dependent factor of change Δh_k is applied to the hazard intensity as (Kirezci et al. 2020):

$$h_k = h_k^0 + \Delta h_k \tag{11}$$

It is worth mentioning that the present hazard model does not account for the temporal dependence across successive DEs. This may limit its applicability to hazards exhibiting clustering and seasonality. For such cases, more advanced approaches would be required to represent non-stationarity in both DE characteristics and their temporal occurrence (Nayak et al. 2024).

2.3. *Budget allocation optimization*

In this work, the budget allocation problem is defined as a Sequential Decision Problem (SDP) characterized by the set $\Sigma, \mathrm{A}, \Pi, \mathcal{R}, \gamma$, where (Sutton and Barto 2018):

- Σ is the state space (i.e., the set of all possible system states, where each state is a vector of variables that fully describes the state of the system);
- A is the action space (i.e., the set of possible investments);
- Π is the set of transition probabilities (i.e., $\pi(\sigma_{k+1}|\sigma_k, \alpha) \in \Pi$ is the probability to make a transition from state σ_k to state σ_{k+1} when an action α is performed);
- $\mathcal{R}$ is the reward function (i.e., $\mathcal{R}(\sigma_{k+1}|\sigma_k, \alpha)$ is the reward corresponding to the state change from σ_k to σ_{k+1} because of α);
- $\gamma \in [0,1]$ is the discount factor, which is used to evaluate the present value of future rewards.

The SDP aims at finding the optimal investment policy, which determines, for each state σ, the sequence of actions to be adopted at each decision time T_k to maximize the reward over the mission time T_M. Since resilience investments must reflect decision-maker preferences, their optimal allocation depends on how different infrastructure commodities (e.g., electricity and gas) and impacts (i.e., social and economic) are valued. To capture this, the proposed framework uses a multi-criteria preference structure, defined through a set of normalized weights w_i associated with different commodities and, for each commodity, a set of impact-specific normalized weights w_{ip}. For the sake of simplicity, the dependence from the hazard intensity H is omitted in what follows. These weights are embedded in the reward function of the SDP, defined as:

$$\mathcal{R}(\sigma_{k+1}|\sigma_k,\alpha) = \sum_{i=1}^{I} w_i \sum_{p=1}^{P} w_{ip}\, \Delta\bar{\mathcal{J}}_{ip}\,(\sigma_{k+1}|\sigma_k) - \Gamma(\alpha) \tag{12}$$

where $\Gamma(\alpha)$ is the cost of action α and $\Delta\bar{\mathcal{J}}_{ip}(\sigma_{k+1}|\sigma_k)$ is the difference between the expected *p-th* impact of the *i-th* commodity between system states σ_k and σ_{k+1} (i.e., the change due to action α). The impacts $\mathcal{J}_{ip}(\sigma)$ are defined as follows:

- social impact: $\mathcal{J}_{i1}(\sigma) = D_{i1}(\sigma)$, representing the disruption experienced by residential consumers;
- economic impact: $\mathcal{J}_{i2}(\sigma) = \frac{D_{i1}(\sigma)+D_{i2}(\sigma)}{2}$, representing the aggregated disruption experienced by both residential and industrial consumers.

Each expected impact $\bar{\mathcal{J}}_{ip}(\sigma_k)$ is estimated with a Monte Carlo simulation with N_{MCS} trials, sampling the hazard magnitude and duration and the CIs nodes failures and repair times and the SDP is solved by Proximal Policy Optimization (PPO) (Schulman et al. 2017).

3. Case study

The framework of Section 2 is applied to a simplified model of the gas and electric network of Houston, Texas, USA, exposed to frequent costal floodings caused by the combination of extreme rainfall and storm surge during hurricanes (Valle-Levinson, Olabarrieta, and Heilman 2020). Moreover, the future vulnerability of this region to costal floods is exacerbated by the projected Sea Level Rise (SLR) due to CC (Miller and Shirzaei 2021) and by the concurrent inland subsidence due to groundwater and oil and gas extraction (Coplin and Galloway 1999). The considered time horizon of the budget allocation problem for resilience improvement is from 2025 to $T_M = 2100$ with five years intervals between investments, for a total of $K = 15$ sequential decisions.

3.1. *CIs model*

Fig. 1 shows the CI systems under study and their interdependency (i.e., interlayer edges), represented by the link between the substations, which supply electricity, and compressors, which are used to transport gas. Supplier nodes (29) include fossil generation units (i.e., a coal plant (1) and gas plants (9)), a gas hub (1), compressors (9) and renewable generation units (i.e., wind farms (3) and solar farms (6)), whereas consumer nodes (9) are modeled as county level electrical distribution stations (Global Energy Monitor 2026). To estimate floodwall investment costs, land use requirements are approximated by a scaling factor that accounts for power capacity and asset type (Stevens 2017). Also, county level residential and industrial demands are scaled according to population and number of power plants, respectively (U.S. Energy Information Administration 2025; GridInfo n.d.).

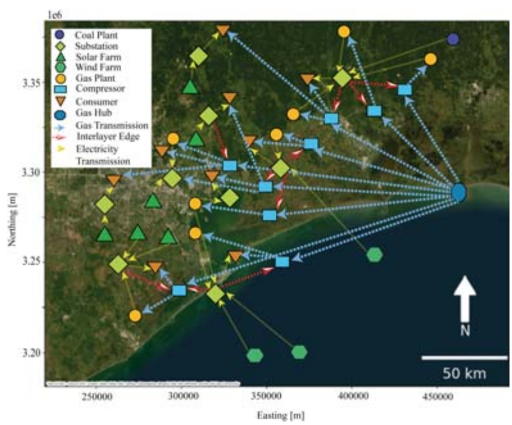

Fig. 1. Case study.

For illustrative purposes and without loss of generality, the probability of failure of each supplier node is modelled by a lognormal fragility PDF in terms of the hazard intensity measure, i.e., inundation depth, with mean θ^f and standard deviation σ^f listed in Table 1.

Table 1. Fragility Distributions Parameters for each asset type in terms of inundation depth (meters).

Asset type	θ^f	σ^f
Solar farm	1.0	0.5
Substation	3.0	0.20
Compressor	3.0	0.20
Coal plant	5.0	0.30
Gas plant	8.0	0.30

Repairs are modeled using unit dependent piecewise constant mean repair times, μ_r, that vary based on unit structural complexity and inundation depth intensity (see Table 2). Particularly, substations and compressors use baseline repair times, whereas thermal and solar units are scaled by factors of 1.5 and 0.8, respectively (Espinoza et al. 2020; Movahednia and Kargarian 2022; Rahman et al. 2020). These assumptions hold: *i)* constant population and power demand over T_M, *ii)* wind farms and the gas hub are considered invulnerable *iii)* consumer nodes do not directly fail.

Table 2. Mean repair time μ_r (hours) by asset type and inundation depth (meters).

Asset type	Inundation depth interval				
	(0 0.5]	(0.5 0.6]	(0.6 0.8]	(0.8 0.9]	> 0.9
Solar farm	10	11	14	16	20
Substation	12	14	18	19	25
Compressor	12	14	18	19	25
Coal plant	19	21	27	29	38
Gas plant	19	21	27	29	38

3.2. *Hazard model*

Historical data are extracted from National Oceanic and Atmospheric Administration (NOAA) gauge station 8770777 Manchester, TX (NOAA accessed Jan. 16, 2025). Water level time series from 1950-08-01 to 2025-07-31 (hourly sampled) are elaborated with a peak over threshold methodology to extract flood data, by employing a threshold of $\mu = 1.405$ meters above NAVD88A (corresponding to a medium inundation level). The two parameters Generalized Pareto Distribution (GPD) is used to fit the marginal CDF of $F_H(h)$ (Han et al. 2018):

$$F_H(h) = 1 - \left\{1 + \left[\frac{\xi(h-\mu)}{\beta}\right]\right\}^{-\frac{1}{\xi}} \qquad (13)$$

where ξ and β are the GPD shape and scale parameters, respectively. Instead, a gamma distribution is used to fit the marginal CDF of $F_{T_H}(t_h)$. The estimated parameters of the marginals are listed in Table 3 along with the corresponding Kolmogorov-Smirnov (KS) test statistics.

Table 3. Marginal distributions parameters.

Variable	ξ	β	KS	p-value
H	0.801	0.195	0.149	0.605
T_H	0.783	15.484	0.162	0.503

To assess the dependence between H and T_H two rank correlation statistics are calculated, namely the Spearman rho ρ_S and the Kendall tau τ, which suggest a high degree of positive correlation (Table 4).

Table 4. Rank correlation between H and T_H (bootstrap percentile confidence interval $Q_{0.05} - Q_{0.95}$ is estimated with 5000 resamples).

Statistic	Estimate	$Q_{0.05}$	$Q_{0.95}$
ρ_S	0.908	0.797	0.967
τ	0.765	0.590	0.872

A set of three Archimedean copulas families are fitted to the historical data and are evaluated with respect to their log-likelihood $\ln(\mathcal{L})$, their Akaike Information Criteria (AIC) and their Bayesian Information Criteria (BIC) (Table 5). The Gumbel copula is selected due to the highest $\ln(\mathcal{L})$ and lowest AIC and BIC.

Table 5. Estimated copula parameters.

Family	ϑ	$\ln(\mathcal{L})$	AIC	BIC
Gumbel	3.816	20.108	-38.216	-37.038
Frank	13.392	19.412	-36.824	-35.646
Clayton	4.014	17.559	-33.118	-31.942

The effect of time dependent CC is introduced by considering the SLR projections from IPCC6 (Fox-Kemper et al. 2021; Kopp et al. 2023, Garner et al. 2021). Thus, for any k-th decision time, the additive correction factor Δh_k, is calculated as:

$$\Delta h_k = SLR_k + \Delta sub\ (T_{k+1} - T_k) \qquad (14)$$

Where Δsub denotes the land subsidence, which for the Houston Bay area is estimated as 6.7 mm/year (Buzzanga et al. 2025). For any realization of (h_k, t_{hk}) the Height Above Nearest Drainage (HAND) methodology (Zheng et al. 2018) is used to derive a spatial map of the inundation level in correspondence of each node of the CIs.

3.3. *Sequential Decision Problem*

The SDP for the considered case study is defined as follows:

- State space: at each decision time T_k, the system state is characterized by $\boldsymbol{\sigma}_k = [\boldsymbol{O}_k, \Delta h_k^*, \boldsymbol{w}_k^*]$, where $\boldsymbol{O}_k = [O_{k1}, \dots, O_{kn^c}, \dots, O_{kN^c}]$, with $N^c = N_1^c \cup N_2^c$, is the vector of the current flood wall heights for each non-consumer node in the CIs, $\Delta h_k^* = \Delta h_k + \epsilon_{kh}$ is the noisy measure of the hazard intensity change due to sea level rise and land subsidence, with $\epsilon_{kh} \sim N(0, 0.02\Delta h_k)$ and $\boldsymbol{w}_k^* = [w_{k1}^*, w_{k2}^*, w_{k11}^*, w_{k12}^*, w_{k21}^*, w_{k22}^*]$ is the noisy vector of the preference weights, where each $w_k^* = w_k + \epsilon_{kw}$ with $\epsilon_{kw} \sim N(0, 0.1\mathrm{w_k})$;
- Action space: the considered investments are discrete increases of the floodwall heights. The action at decision time k is then characterized by the vector $\boldsymbol{\alpha}_k = [\Delta O_{k1}, \dots, \Delta O_{kn^c}, \dots, \Delta O_{kN^c}]$, containing the discrete wall increases for each non-consumer node in the CIs. The discrete values considered are $\Delta O_k \in [0, 0.5, 1, 1.5, 2, 2.5, 3]\ m$ and the associated cost is calculated as follows:

$$\Gamma(\Delta O_{kn^c}) = \Delta O_{kn^c}\, L_{n^c}\, \Gamma_{wall} \qquad (15)$$

  where L_{n^c} is the perimeter of the n^c-*th* non-consumer node and $\Gamma_{wall} = 3.31 \frac{M€}{km\, m}$ is the unit cost per km of floodwall and meter of heightening (Aerts et al. 2013);
- Transition probabilities: we consider each action to have a deterministic effect on the system, which is an increase in the floodwalls height, leading to an updated state from decision time k to $k+1$ equal to $\boldsymbol{\sigma}_{\boldsymbol{k+1}} = [\boldsymbol{O}_{k+1}, \Delta h_{k+1}^*, \boldsymbol{w}_{k+1}^*]$, where $\boldsymbol{O}_{k+1} = \boldsymbol{O}_k + \boldsymbol{\alpha}_k$, $\Delta h_{k+1}^* = \Delta h_{k+1} + \epsilon_{(k+1)h}$ and $\boldsymbol{w}_{k+1}^* = \boldsymbol{w}_{k+1} + \boldsymbol{\epsilon}_{(k+1)w}$ are the updated preferences as described in Fig. 2.
- Reward calculation: the reward is calculated modifying Eq. (11) adding a penalty term to avoid overbudget P_b and a penalty term to avoid consecutive improvements of the same node P_c:

$$\mathcal{R}^P(\sigma_{k+1}|\sigma_k, \alpha) = \mathcal{R}(\sigma_{k+1}|\sigma_k, \alpha) - P_b - P_c \qquad (16)$$

  P_b and P_c are equal to 1 if the total cost of an action is larger than the budget $B = 50\ M€$ and if consecutive improvements are present, respectively. To estimate the expected impacts, $N_{MCS} = 10^4$ Monte Carlo trials are used.

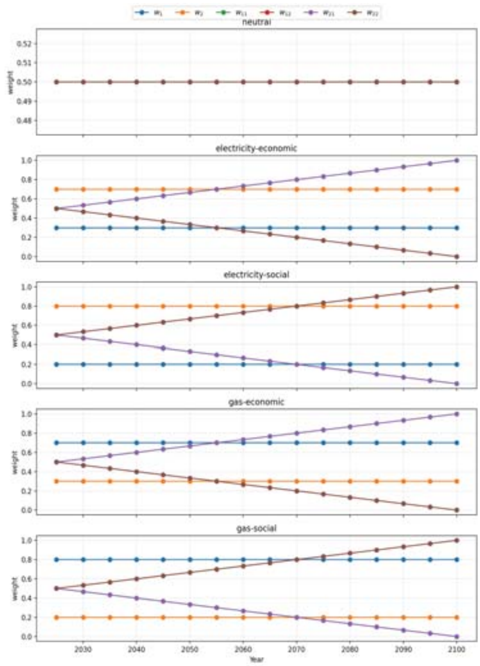

Fig. 2. Decision maker preferences scenarios.

4. Results

The framework presented in Section 2 has been applied to the case study of Section 3. The following hyperparameters have been used for the PPO:

- actor and critic models: multi-layer perceptron with two hidden layers of 128 neurons each and a learning rate $lr = 5 \cdot 10^{-4}$;
- discount factor $\gamma = 0.99$;
- clipping parameter $\epsilon = 0.2$;

The agent has been trained until convergence of the reward, and it has been tested using the SLR projections from the SSP5-8.5 scenario and the weights of Fig. 3, unseen during training, in which the decision maker preferences switch from gas to electricity after the first 30 years.

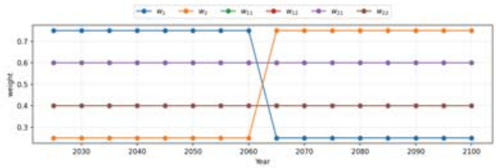

Fig. 3. Test decision maker preferences.

The test results have been compared with a benchmark expert-based policy, in which the budget is always divided equally among the three most fragile assets at each decision time, in terms of expected gas and electricity supply. As shown in Fig. 4, the DRL agent (blue line) outperforms the expert-based policy (orange line) for both commodities during the whole life of the system. Also, as shown in Table 5, the cumulative expenditures correctly shift from gas to electricity after the first 30 years, following the evolving preferences of the decision maker.

Table 5. Expenditures per commodity.

Asset type	Period	Expenditure
Gas	$\leq$ 30 years	€ 15.0 MM
	> 30 years	€ 0.75 MM
Electricity	$\leq$ 30 years	€ 12.5 MM
	> 30 years	€ 20 MM

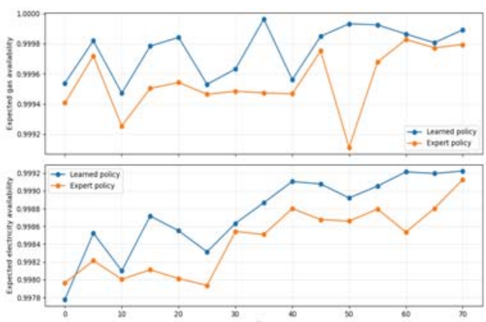

Fig. 4. Comparison of learned and expert policy.

5. Conclusions

This work introduces a DRL-based sequential decision-making framework for resilience investment planning in the context of interdependent CIs exposed to natural hazards. The resilience budget allocation problem is formulated as an SDP, enabling the explicit representation of non-stationary hazard conditions and time-varying stakeholder preferences. The application to an integrated power-gas network exposed to coastal flooding shows that the proposed method consistently outperforms an expert-based benchmark, while dynamically reallocating investments in response to changes in hazard intensity and stakeholder preferences. These findings highlight the flexibility and robustness of the proposed framework for CIs resilience-oriented decision making under CC uncertainty. Future work will be aimed at relaxing simplifying assumptions in the CI modeling and extending the framework to account for multiple hazards, time-dependent evolution of the network topology (including the introduction of new asset types), projected demographic dynamics during the investment horizon and multiple potentially conflicting stakeholders, thereby further enhancing its applicability to realistic resilience investment planning scenarios.

Acknowledgement

The work of Santiago Taguado Menza is supported by the Italian Ministry of University and Research (MUR/MIUR, PRIN 2022 Program) and by the European Union's NextGenerationEU initiative under Grant No. 2022TAFXZ5, within the project ARISTOTELES (ARtificial Intelligence and STOchasTic simulation for the rEsiLience of critical infrastructurES). The work of Thomas Matteo Coscia is supported by PE RETURN SPOKE VS4 (CUP D43C22003030002, codice progetto PE0000005), for the project titled "MULTI RISK SCIENCE FOR RESILIENT COMMUNITIES UNDER A CHANGING CLIMATE", funded by the NextGenerationEU – Piano Nazionale di Ripresa e Resilienza (PNRR) (Missione 4, componente 2, Investimento 1.3). We thank the projection authors for developing and making the sea-level rise projections available, multiple funding agencies for supporting the development of the projections, and the NASA Sea-Level Change Team for developing and hosting the IPCC AR6 Sea-Level Projection Tool. We acknowledge the CINECA award under the ISCRA initiative, for the availability of high performance computing resources and support.

The authors thank the organizers of the *1st Young Researcher Bilateral Workshop on Reliability & Risk Assessment in Uncertain Environments* and the supporting institutions (Politecnico di Milano, the European Safety and Reliability Association (ESRA) and Leibniz Universität Hannover) for providing the forum and support for presenting the conceptualization of this work. The authors also acknowledge Professor Giovanni Sansavini (ETH) and Professor Ibrahim

Ahmed (POLIMI) for their guidance in the conceptualization of this study.

References

Aerts, Jeroen C. J. H., W. J. Wouter Botzen, Hans de Moel, and Malcolm Bowman. 2013. "Cost Estimates for Flood Resilience and Protection Strategies in New York City." *Annals of the New York Academy of Sciences* 1294: 1–104.

Buzzanga, B., M. Govorcin, F. Kremer, J. E. Schubert, D. P. S. Bekaert, B. Schaeffer, P. Milillo, et al. 2025. "Satellite-Based Vertical Land Motion for Infrastructure Monitoring: A Prototype Roadmap in Greater Houston, Texas." *Scientific Reports* 15: 17041.

Clavijo Mesa, Maria Valentina, Francesco Di Maio, and Enrico Zio. 2025. "Dynamic Inoperability Input-Output Modeling of a System of Systems Made of Multi-State Interdependent Critical Infrastructures." *Reliability Engineering & System Safety* 264: 111303.

Coplin, Laura S., and Devin L. Galloway. 1999. "Houston-Galveston, Texas: Managing Coastal Subsidence." In *Mining Ground Water*, 35–48.

Espinoza, Sebastián, Alan Poulos, Hugh Rudnick, Juan Carlos de la Llera, Mathaios Panteli, and Pierluigi Mancarella. 2020. "Risk and Resilience Assessment with Component Criticality Ranking of Electric Power Systems Subject to Earthquakes." *IEEE Systems Journal*.

Fang, Yi-Ping, Giovanni Sansavini, and Enrico Zio. 2019. "An Optimization-Based Framework for the Identification of Vulnerabilities in Electric Power Grids Exposed to Natural Hazards." *Risk Analysis* 39 (9): 1949–69.

Fox-Kemper, Baylor, Helene T. Hewitt, C. Xiao, G. Aðalgeirsdóttir, S. S. Drijfhout, T. L. Edwards, N. R. Golledge, et al. 2021. "Ocean, Cryosphere and Sea Level Change." In *Climate Change 2021: The Physical Science Basis. Contribution of Working Group I to the Sixth Assessment Report of the Intergovernmental Panel on Climate Change*, edited by V. Masson-Delmotte, P. Zhai, A. Pirani, S. L. Connors, C. Péan, S. Berger, et al., 1211–1362. Cambridge: Cambridge University Press. https://doi.org/10.1017/9781009157896.011.

Garner, Gregory G., Thomas Hermans, Robert E. Kopp, Aimée B. A. Slangen, T. L. Edwards, Anders Levermann, S. Nowicki, et al. 2021. *IPCC AR6 Sea Level Projections*. Version 20210809. Dataset. Zenodo. Accessed January 19, 2026.

Global Energy Monitor. n.d. "Global Energy Monitor." Accessed January 19, 2026.

GridInfo. n.d. "GridInfo." Accessed January 19, 2026.

Han, Chao, Shuguang Liu, Yiping Guo, Hejuan Lin, Yuyin Liang, and Hong Zhang. 2018. "Copula-Based Analysis of Flood Peak Level and Duration: Two Case Studies in Taihu Basin, China." *Journal of Hydrologic Engineering* 23 (6): 05018009. https://doi.org/10.1061/(ASCE)HE.1943-5584.0001661.

Kirezci, Ebru, Ian R. Young, Roshanka Ranasinghe, Sanne Muis, Robert J. Nicholls, Daniel Lincke, and Jochen Hinkel. 2020. "Projections of Global-Scale Extreme Sea Levels and Resulting Episodic Coastal Flooding over the 21st Century." *Scientific Reports* 10: 11629.

Kopp, Robert E., Gregory G. Garner, Thomas H. J. Hermans, Shubham Jha, Praveen Kumar, Andrew Reedy, Aimée B. A. Slangen, et al. 2023. "The Framework for Assessing Changes To Sea-Level (FACTS) v1.0: A Platform for Characterizing Parametric and Structural Uncertainty in Future Global, Relative, and Extreme Sea-Level Change." *Geoscientific Model Development* 16: 7461–7489.

Liang, Huangbin, Beatriz Moya, Francisco Chinesta, and Eleni Chatzi. 2026. "Resilience-Based Post Disaster Recovery Optimization for Infrastructure System via Deep Reinforcement Learning." *Reliability Engineering & System Safety* 265: 111478.

Miller, Megan M., and Manoochehr Shirzaei. 2021. "Assessment of Future Flood Hazards for Southeastern Texas: Synthesizing Subsidence, Sea-Level Rise, and Storm Surge Scenarios." *Geophysical Research Letters* 48: e2021GL092544.

Movahednia, Mohadese, and Amin Kargarian. 2022. "Flood-Aware Optimal Power Flow for Proactive Day-Ahead Transmission Substation Hardening." arXiv:2201.03162.

Nayak, A., Gentine, P., & Lall, U. 2024. "A nonstationary stochastic simulator for clustered regional hydroclimatic extremes to characterize compound flood risk." *Journal of Hydrology X*, 25, 100189.

National Oceanic and Atmospheric Administration. n.d. "Tides & Currents: Station 8770777 (Manchester, TX)—Water Levels." Accessed January 19, 2026. https://tidesandcurrents.noaa.gov/waterlevels.html?id=8770777.

Nozhati, Saeed. 2021. "A Resilience-Based Framework for Decision Making Based on Simulation-Optimization Approach." *Structural Safety* 89: 102032.

Nozhati, Saeed, Yugandhar Sarkale, Edwin K. P. Chong, and Bruce R. Ellingwood. 2020. "Optimal Stochastic Dynamic Scheduling for Managing Community Recovery from Natural Hazards." *Reliability Engineering & System Safety* 193: 106627.

Ouyang, Min. 2014. "Review on Modeling and Simulation of Interdependent Critical Infrastructure Systems." *Reliability Engineering & System Safety* 121: 43–60.

Rahman, Shams A., Alex G. D. McLellan, John Taylor, and Neil R. Osborne. 2020. *Compressor Station Facility Failure Modes and Related Effect Analysis for CO_2 Pipeline Quantitative Risk Assessment*. Luxembourg: Publications Office of the European Union. https://doi.org/10.2760/67609.

Salvadori, G., and C. De Michele. 2004. "Frequency Analysis via Copulas: Theoretical Aspects and Applications to Hydrological Events." *Water Resources Research* 40: W12511.

Schulman, John, Filip Wolski, Prafulla Dhariwal, Alec Radford, and Oleg Klimov. 2017. "Proximal Policy Optimization Algorithms." arXiv:1707.06347 (cs.LG).

Stevens, Landon. 2017. *The Footprint of Energy: Land Use of U.S. Electricity Production*. Report. Strata Policy, June 2017.

Sutton, Richard S., and Andrew G. Barto. 2018. *Reinforcement Learning: An Introduction*. 2nd ed. Cambridge, MA: The MIT Press. http://incompleteideas.net/book/the-book-2nd.html.

U.S. Energy Information Administration. 2025. "Texas: State Profile and Energy Estimates." Accessed January 19, 2026. https://www.eia.gov/beta/states/states/tx/overview.

Valle-Levinson, Arnoldo, Maitane Olabarrieta, and Lorraine Heilman. 2020. "Compound Flooding in Houston–Galveston Bay during Hurricane Harvey." *Science of the Total Environment* 747: 141272.